23rd International Conference on Renewable Energies and Power Quality (ICREPQ'25)
Tenerife (Spain), 25th to 27th June 20245
Renewable Energy and Power Quality Journal (RE&PQJ)
ISSN 2172-038 X, Volume No.23, September 2025

The use of GIS as a tool for the integrated design of solar photovoltaic street lighting systems

Ovidio Rabaza, Evaristo Molero, Antonio Peña-García

Department of Civil Engineering. University of Granada, 18071, Granada, Spain

Abstract. The integrated design of solar street lighting based on Geographic Information Systems (GIS) is an innovative approach that combines solar technologies and spatial analysis to optimize stand-alone photovoltaic street lighting installations. This work presents a GIS-based tool in the prototype phase for automated urban planning, enabling the rapid and accurate design of solar public lighting across all streets simultaneously in rural, residential, or urban areas. Designing an installation of this kind for a single street is a time-consuming task, and when multiple streets are involved, the process becomes significantly more complex. To address this, the project integrates a GIS model that streamlines the large-scale design and planning process. The model incorporates relevant geospatial data, including location, road width, solar irradiation levels, required lighting levels, shaded areas, and luminaire catalogues. This tool considers lighting requirements based on safety standards and community needs, adjusting the arrangement of luminaires, battery capacity, and panel power to ensure the system is solar-powered and capable of delivering the intended service.

Key words. PV battery system, street lighting, GIS.

1. Introduction

Solar energy is becoming increasingly important as an accessible energy source due to its sustainability and non-polluting nature, especially in rural and remote regions [1], where electricity generation capacity is limited. Decentralized PV generation [2] has been shown to be an efficient and cost-effective option, reducing losses, increasing efficiency, providing greater energy independence, and lowering costs [2].

In rural areas, where high levels of lighting are unnecessary due to low motor vehicle traffic, protection from light pollution [3], or the difficulty and high cost of accessing the electricity grid [4], LED luminaires provide higher efficiency and lower energy consumption compared to traditional discharge lamps [5]. As a result, solar public lighting with LED technology is considered the most economical and practical option for remote locations where ensuring lighting is essential for safety and facilitating traffic.

Some initiatives in the literature address models for designing solar street lighting installations, focusing on the optimal sizing of renewable energy systems for these applications. Notable examples include the studies by [6], [7], which present a case study centered on the energy aspect—specifically the PV/battery system—where genetic algorithms are applied as an optimization technique. Similarly, [8] conducted a techno-economic analysis of street lighting installations powered by photovoltaic systems. The models were developed using HOMER software [9], and, as in the previous example, optimization focused solely on the photovoltaic/battery system.

In both examples, the lighting design was conducted independently of the energy system and applied to a single street or road. When designing lighting for multiple streets with corresponding renewable energy systems, the calculations increase, as the streets are likely to differ in geometry and lighting requirements. To address this challenge, the researchers of this article propose using tools that enable large-scale design, such as Geographic Information Systems (GIS).

Geographic Information Systems (GIS) are widely recognized tools for providing large-scale geospatial information. One of their primary functions is to support decision-making by offering a spatial perspective on data. GIS has numerous applications, including urban planning, where it aids in the efficient management of urban resources such as public lighting installations.

The use of GIS in street lighting can offer several benefits for municipal authorities, utilities, and other stakeholders involved in managing rural or urban lighting. When combined with renewable energy resource data, GIS becomes a powerful tool for reducing the design time of renewable energy-powered installations.

For this reason, this work develops a GIS model for designing a complete solar street lighting installation. The accuracy of the results will then be validated through a practical example using two computer applications—one focused on lighting and the other on designing photovoltaic solar energy-powered installations.

2. Materials and method

In this work, QGIS software [10] is used to calculate, analyse, and edit the spatial information of the map. Various geo-referenced layers display the optimal installation arrangements, battery capacity, peak power of the photovoltaic module, pole spacing, and luminaire height, all based on optimization criteria. Python, along with libraries such as *scipy.optimize*, is employed to integrate optimization algorithms that generate optimal solutions.

The version of QGIS software used in this article is 3.38.3 (Grenoble).

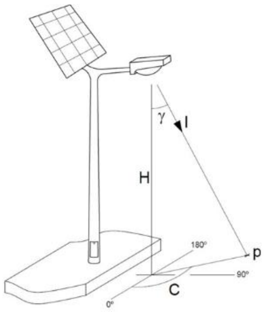

γ	C0°	C5°	C10°	C80°
0°	334.18	334.18	334.18	334.18
5°	334.18	335.35	336.33	341.99
10°	334.18	336.52	338.09	340.43
15°	333.69	337.11	339.55	336.04
⋮	⋮	⋮	⋮	⋮
70°	351.95	633.62	705.75	21.96

Fig. 1. Example of luminous intensity table (right) of the luminaire according to the *C*-*γ* system (left).

A. Public lighting

Considering that the primary objectives of public lighting installations are safety, visibility [11], and sustainability, the most critical design parameters include lighting levels, quality, and power consumption.

Based on the characteristics of these installations and the properties of the luminaires provided by manufacturers, the formula used to calculate lighting levels is the illuminance at any point p on the roadway:

$$E(p) = \frac{\Phi}{1000} \cdot \frac{I(C,\gamma)}{H^2} \cdot cos^3\gamma \ [lux] \quad (1)$$

where H is the mounting height of the luminaire, Φ represents the luminous flux (lm) of the lamp, and I(C,γ) is the luminous intensity (cd/klm) emitted by the luminaire at an azimuthal angle C and a vertical angle γ (see Fig. 1).

The average illuminance value E_{av} is calculated across the entire roadway using a sampling grid of 10×3 points within the area bounded by a lane and two consecutive luminaires. This method is common and widely accepted [11], [12].

In terms of installation quality, the most important design parameter is overall uniformity, defined as follows:

$$U_0 = \frac{E_{min}}{E_{av}} \quad (2)$$

This parameter measures the homogeneity of lighting across the entire roadway.

Finally, power consumption is linked to lighting levels through *SLEEC* (Street Lighting Energy Efficiency Criterion) or the *Power Density* indicator, defined as [14], [15], [16].

$$SE = \frac{P}{A \cdot E_{av}} \ [W \ m^{-2} \ lux^{-1}] \quad (3)$$

where P is the electrical power of the luminaire, A is the area between two consecutive luminaires and the width of the roadway, and E_{av} is the average illuminance on the roadway.

B. PV-Battery system

Solar photovoltaic street lighting systems consist of a photovoltaic module, LED lamp, maintenance-free sealed monoblock stationary battery, charge regulator, and pole [17]. Additionally, most systems include a twilight sensor to automate switching and optimize power consumption.

The following equations are typically used to calculate the battery capacity and the peak power of the solar panel:

$$C_{Batt} = \frac{DoA \cdot E_D}{DoD \cdot \eta} \ [Wh] \quad (4)$$

$$P_{PV} = \frac{E_D}{SF \cdot LF \cdot PSH} \ [W] \quad (5)$$

Where *DoA* is the number of days of autonomy, E_D is the daily energy consumed by the luminaire, *DoD* is the depth of discharge, η represents the efficiency of the charge controller and battery, *PSH* is the Peak Sun-Hours, *SF* is the shading factor, and *LF* is the loss factor. The loss factor accounts for module temperature rise, soiling, cables losses, battery inefficiencies, module degradation, and the incident angle modifier.

C. Model

The inverse of the SLEEC indicator can be expressed as a function of the road width ω and the luminaire height H using a second-order polynomial [13]:

$$\frac{A \cdot E_{av}}{P} = a_0 + a_1 \frac{\omega}{H} + a_2 \left(\frac{\omega}{H}\right)^2 \equiv P_N \quad (6)$$

Where the coefficients a_0, a_1 and a_2 are characteristic parameters of each Luminaire. Eq. 6 is key to directly relating lighting parameters to energy parameters.

The energy E_D consumed by each luminaire is the product of its electrical power and the hours it operates. Consequently, using Eq. 6, the battery capacity and the peak power of the solar module can be expressed as a function of the parameters defining the lighting installation — E_{av}, H, and S — as follows:

$$C_{Batt} = \frac{DoA \cdot S \cdot \omega \cdot E_{av} \cdot h}{DoD \cdot \eta \cdot P_N} \ [Wh] \quad (7)$$

$$P_{PV} = \frac{S \cdot \omega \cdot E_{av} \cdot h}{SF \cdot LF \cdot PSH \cdot P_N} \ [W] \quad (8)$$

where h is the maximum number of hours the luminaires will be on.

D. Algorithm optimization

The optimization algorithm, developed in Python, follows the sequence of operations illustrated in Figure 2. The input data is divided into two groups: parameters related to regulations and the environment — E_{min}, ω, DoA, DoD, SF, LF, PSH, η and h_{max} — and luminaire-specific data — a_0, a_1, and a_2 — which define energy performance through the P_N polynomial.

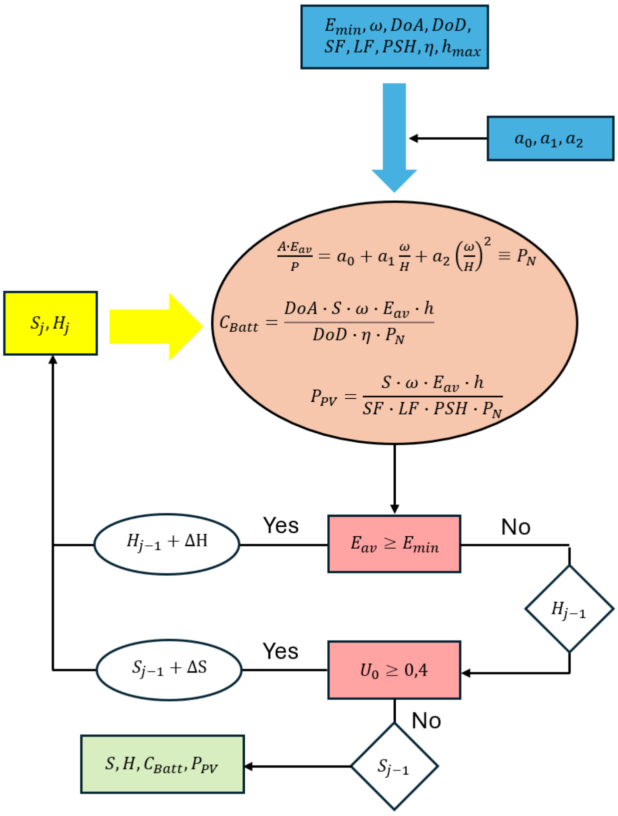

Fig. 2. Flowchart of the optimization algorithm.

The optimization criterion aims to minimize the number of poles by maximizing the spacing between lighting points.

3. Simulation and discussion

The model was applied to a road classified under the CE lighting class, designed for use in urban and rural areas. This classification considers various users, including motor vehicle drivers, cyclists, pedestrians, and the increasingly common electric scooter riders.

A. Input parameters

The road is in southern Spain, within an urbanization in the town of Otura, a village in the province of Granada. It spans 3 km in length and 6 meters in width, with two lanes in both directions. The lighting parameters for the installation are as follows:

Table I. - Type Sizes

Lighting Class	*C4*
E_{av}	$\geq$ *10 lux*
U_0	$\geq$ *0.4*

The luminaire used in the design (Fig. 3) has a power of 20.5 W. Its characteristic coefficients are a_0 = *-0.9109*, a_1 = *84.579*, and a_2 = *-94.92*.

The parameters considered for sizing the PV/battery system are as follows:

Table II. - Type Sizes

PSH	2.33 h
h_{max}	15 h
DoA	2 days
DoD	80 %
η_{batt}	85 %
SF	1
LF	0.75

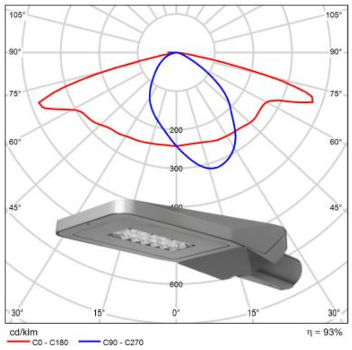

Fig. 3. Street lighting Led luminaire and its polar diagram.

B. Lighting and PV/Battery optimal design

After executing the script in the QGIS Python console, the layout, luminaire spacing, luminaire height, minimum battery capacity, and peak power of the PV module were calculated. The resulting design is shown in Figure 4.

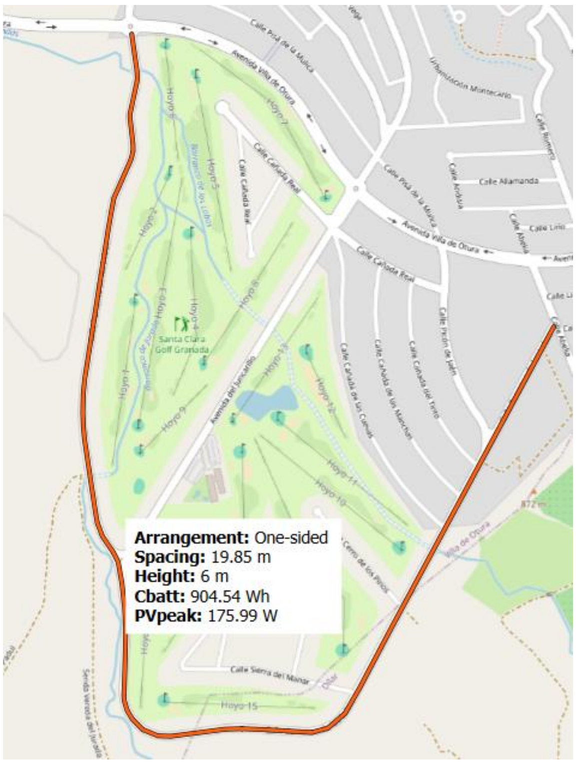

Fig. 4. Result of the installation design generated by QGIS

To verify that the results obtained with the GIS-based model meet expectations, two checks were performed. First, the optimal arrangement of the luminaires was calculated to ensure the required lighting levels. Second, it was confirmed that the calculated PV/battery system could supply the energy necessary for the installation's operation. The lighting was validated using DIALux software [14], with the results shown in Figure 5.

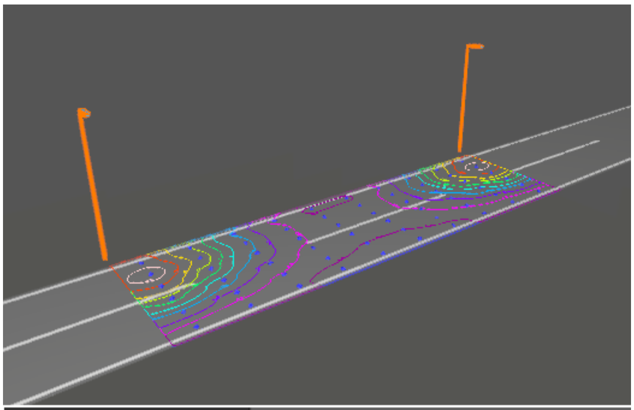

Maintenance factor	0.800
Luminaire arrangement 1	BRISA-L2WG6-LC-W1-24LED-4000K-3240LM-2
Fitting	24 x LED
Pole distance [m]	19.850
Light centre height [m]	6.000
Boom angle [°]	0.0
Wattage / route [W/km]	1025
D_p [W/(lx*m²)]	0.017
E_m [lx]	✓ ≥ 10.00 — 10.10 ✓
U_o	✓ ≥ 0.40 — 0.54 ✓

Fig. 5. Example of luminous intensity table (right) of the luminaire according to the C-γ system (left).

As demonstrated, the calculation performed by DIALux confirms that the optimal lighting design involves spacing the luminaires 19.85 meters apart with a height of 6 meters, consistent with the results obtained using QGIS. Additionally, the illuminance and uniformity levels meet the requirements of the specified lighting class, achieving an average illuminance of 10.1 lx and a uniformity of 0.54.

A subsequent test was conducted using PVGIS [15], a free online photovoltaic calculation tool. The location of the installation, the module power, the battery capacity, and the luminaire's energy consumption during the longest night of the year were input into the application for evaluation.

Fig. 6 illustrates the data entered into the free online PVGIS application. Based on the results obtained from QGIS, a minimum battery capacity of 904.54 Wh and a module power of 176 W are required to power the luminaire, assuming a maximum operating time of 15 hours during December (see Table II). Given that the luminaire's power consumption is 20.5 W, its highest daily energy consumption is estimated at 307.5 Wh.

Provided inputs:	
Location [Lat/Lon]:	37.079,-3.635
Horizon:	Calculated
Database used:	PVGIS-ERA5
PV installed [Wp]:	176
Battery capacity [Wh]:	904.54
Discharge cutoff limit [%]:	40
Consumption per day [Wh]:	307.5
Slope angle [°]:	35
Azimuth angle [°]:	0

Fig. 6. Input data entered into the PVGIS application.

The simulation results provided by PVGIS are presented in Figure 7. This figure depicts the average daily energy production of the PV module, and the average daily energy stored in the battery for each month of the year. As shown in the upper section of Figure 7, the PV module consistently produces surplus energy, as the load consumption (Energy output) is lower than the PV production (Energy output + Energy not captured).

The energy produced daily by the PV modules is stored directly in the battery, which is designed to ensure that the daily depth of discharge does not exceed 40%. This corresponds to a maximum depth of discharge of 80%, considering an autonomy of 2 days.

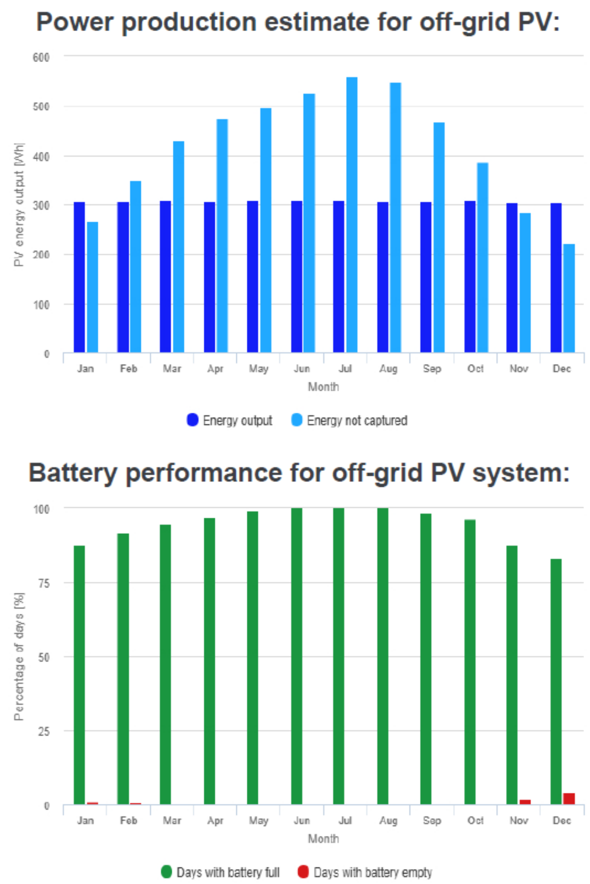

Fig. 7. Power production estimate (upper) and battery performance (lower) for the stand-alone solar street lighting system.

The lower image of Figure 7 illustrates the battery's state of charge throughout the year. December is identified as the most challenging month, given its lower solar radiation and higher energy consumption hours. The results show that on 4.24% of the days in December, the battery reaches or exceeds the daily discharge limit of 40%. This corresponds to a total of approximately 1.3 days during the month. However, the battery never fully depletes, ensuring that the luminaires always remain powered throughout the year.

This is illustrated in Figure 8, which depicts the battery's state of charge at the end of each day (00:00 h).

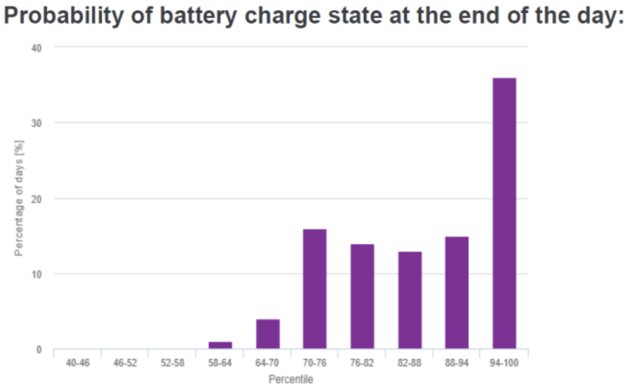

Fig. 8. Percentage of battery charge at the end of the day (x-axis) versus percentage of days per year (y-axis).

According to the results provided by PVGIS and illustrated in Figure 8, there is a 100% probability that the battery will maintain a charge level of at least 58% at the end of each day. This ensures a reliable power supply to the luminaire even under the most challenging conditions, such as during the month with the lowest solar irradiation and the longest night of the year (winter solstice).

C. System cost and LCC analysis

The Life Cycle Cost (LCC) value is calculated as follows:

$$LCC = C_{inv} + \sum \frac{C_{O\&M}}{(1+i)^z} + \sum \frac{C_{rep}}{(1+i)^m} - \frac{RV}{(1+i)^N} \quad (9)$$

where C_{inv} is the sum of the initial costs of purchasing and supplying all system components, as well as the installation costs. $C_{O\&M}$ represents the annual fixed cost of operating and maintaining the facility. z is the number of years the facility operates, set at 25 years in this study. C_{rep} is the cost of replacing the batteries at the end of their life cycle or any other defective component, with replacement occurring m years after the installation of the component to be replaced. RV (recovery value) refers to the value of the facility's components at the end of their use period. Finally, i is the annual interest rate (%).

The result of the economic analysis has been calculated using the studies cited in [7] and is summarized in Table III.

Table III. –Costs considered in the case study of the photovoltaic solar installation in the luminaires.

Item	*Cost*
Installation	*10 %*
O&M	*1 %*
Recovery value	*15 %*
Interest rate	*2 %*
Solar Panel (180 W)	*166 €*
Battery (960 Wh)	*134 €*
Controller (5 A)	*27 €*

Based on this estimate and the associated costs of the photovoltaic (PV) battery system components, the Table IV presents the results of the life-cycle cost (LCC) analysis per kilometer of installation.

Table IV. –LCC analysis per kilometre of solar street installation

Item	*Value*
Initial cost PV/System	*16,474.3 €*
Installation and wiring	*1,647.4 €*
Replaced batteries	*6,750.9 €*
O&M	*164.7 €*
Recovery value	*2,471.1 €*
LCC	**45,702.5 €**

Assuming the luminaires operate for an average of 13 hours per day (ranging from 15 hours in December to 11 hours in June), the annual renewable energy consumption is estimated at 4,900 kWh per kilometer of installation.

This practical example demonstrates the dimensioning of a complete solar photovoltaic lighting installation using QGIS, ensuring the required lighting levels and energy support through renewable sources. While the example focused on a single luminaire, the model can accommodate a wide variety of luminaires and optimizing for the most economically sustainable installation.

The application of GIS in designing such installations enables large-scale dimensioning and offers significant potential, particularly when addressing roads or streets with varying characteristics.

4. Conclusion

This paper presents an innovative GIS-based model for solar photovoltaic lighting design that allows the calculation and optimization of systems dedicated to lighting (layout, pole spacing and luminaire height) as well as those dedicated to renewable power supply (photovoltaic module and battery). Its originality lies in its ability to simultaneously address lighting and energy aspects through renewable sources, offering a holistic approach that contrasts with the traditional and isolated methods found in the existing literature. Furthermore, given the complexity and cost associated with these installations, their implementation through GIS will facilitate data-driven decision making, improving accuracy and reducing risks in their large-scale design.

References

[1] M. Hosenuzzaman, N. A. Rahim, J. Selvaraj, M. Hasanuzzaman, A. B. M. A. Malek, y A. Nahar, «Global prospects, progress, policies, and environmental impact of solar photovoltaic power generation», *Renewable and Sustainable Energy Reviews*, vol. 41, pp. 284-297, ene. 2015, doi: 10.1016/j.rser.2014.08.046.

[2] A. K. Khamis, N. E. Zakzouk, y A. K. Abdelsalam, «Generalized Cost-effective Converter for Solar Street Lighting featuring Averaged State-space Model-based Sensorless MPPT», *Computers and Electrical Engineering*, vol. 101, p. 108004, jul. 2022, doi: 10.1016/j.compeleceng.2022.108004.

[3] A. Peña-García y A. Sędziwy, «Optimizing Lighting of Rural Roads and Protected Areas with White Light: A Compromise among Light Pollution, Energy Savings, and Visibility», *LEUKOS*, vol. 16, n.º 2, pp. 147-156, abr. 2020, doi: 10.1080/15502724.2019.1574138.

[4] R. Ciriminna, F. Meneguzzo, L. Albanese, y M. Pagliaro, «Solar street lighting: a key technology en route to sustainability», *WIREs Energy & Environment*, vol. 6, n.º 2, p. e218, mar. 2017, doi: 10.1002/wene.218.

[5] R. D. Dupuis y M. R. Krames, «History, Development, and Applications of High-Brightness Visible Light-Emitting Diodes», *J. Lightwave Technol.*, vol. 26, n.º 9, pp. 1154-1171, may 2008, doi: 10.1109/JLT.2008.923628.

[6] R. G. Allwyn, R. Al Abri, A. Malik, y A. Al-Hinai, «Economic Analysis of Replacing HPS Lamp with LED Lamp and Cost Estimation to Set Up PV/Battery System for Street Lighting in Oman», *Energies*, vol. 14, n.º 22, p. 7697, nov. 2021, doi: 10.3390/en14227697.

[7] R. G. Allwyn, A. Al-Hinai, R. Al-Abri, y A. Malik, «Optimization and techno-economic analysis of PV/Battery system for street lighting using genetic algorithm – A case study in Oman», *Cleaner Engineering and Technology*, vol. 8, p. 100475, jun. 2022, doi: 10.1016/j.clet.2022.100475.

[8] G. Liu, «Sustainable feasibility of solar photovoltaic powered street lighting systems», *International Journal of Electrical Power & Energy Systems*, vol. 56, pp. 168-174, mar. 2014, doi: 10.1016/j.ijepes.2013.11.004.

[9] «Hybrid Renewable and Distributed Generation System Design Software». Accedido: 19 de diciembre de 2024. [En línea]. Disponible en: https://homerenergy.com/

[10] «QGIS», QGIS. Accedido: 7 de enero de 2025. [En línea]. Disponible en: https://www.qgis.org/

[11] International Commission on Illumination, *Calculation and Measurement of Luminance and Illuminance in Road Lighting*, vol. 140. CIE, 2000.

[12] H.-Y. Chen, A. J.-W. Whang, Y.-Y. Chen, y C.-H. Chou, «The hybrid lighting system with natural light and LED for tunnel lighting», *Optik*, vol. 203, p. 163958, feb. 2020, doi: 10.1016/j.ijleo.2019.163958.

[13] O. Rabaza, D. Gómez-Lorente, F. Pérez-Ocón, y A. Peña-García, «A simple and accurate model for the design of public lighting with energy efficiency functions based on regression analysis», *Energy*, vol. 107, pp. 831-842, jul. 2016, doi: 10.1016/j.energy.2016.04.078.

[14] DIAL GmbH, «DIAL GmbH». Accedido: 19 de diciembre de 2024. [En línea]. Disponible en: https://www.dialux.com/es-ES/

[15] «Photovoltaic Geographical Information System», PVGIS. [En línea]. Disponible en: https://joint-research-centre.ec.europa.eu/photovoltaic-geographical-information-system-pvgis_en